Optics & Laser Technology 147 (2022) 107677

Contents lists available at ScienceDirect

Optics and Laser Technology

journal homepage: www.elsevier.com/locate/optlastec

Experimental revealing of fiber laser soliton build-up activated by shaking-soliton triplets

Yulong Cao [a], Lei Gao [a,*], Stefan Wabnitz [b,c], Zhiqiang Wang [d,e], Qiang Wu [a], Lingdi Kong [a], Ziwei Li [a], Ligang Huang [a], Wei Huang [a], Tao Zhu [a,*]

[a] Key Laboratory of Optoelectronic Technology & Systems (Ministry of Education), Chongqing University, Chongqing 400044, China
[b] Dipartimento di Ingegneria dell'Informazione, Elettronica e Telecomunicazioni, Sapienza Università di Roma, 00184 Rome, Italy
[c] Novosibirsk State University, 1 Pirogova str, Novosibirsk 630090, Russia
[d] Institute of Optics, University of Rochester, Rochester, NY 14627, USA
[e] Advanced Photonic Technology Lab, College of Electronic and Optical Engineering & College of Microelectronics, Nanjing University of Posts and Telecommunications, Nanjing 210023, China

ARTICLE INFO

Keywords:
Ultrafast laser
Build-up process
Shaking-soliton molecule
Relative phase

ABSTRACT

Optimization of self-starting in passively mode-locked optical soliton fiber laser resonators results from a complex transient dynamic involving soliton molecules, soliton-based complexes and supramolecular structures, with particle-like properties. By means of time-stretch dispersive Fourier transform based real-time spectroscopy, we identify a new route to the passive mode-locking of fiber laser solitons. A raised relaxation oscillation stage is followed by the generation of shaking-soliton molecular triplets. The relative phase between satellite and main pulses of shaking soliton triplets evolves chaotically, while the two satellite pulses are orthogonal to each other in their state of polarization. These results provide new perspectives into the soliton formation and the internal dynamics of soliton molecules with higher degrees of freedom.

1. Introduction

Solitons, forming from a stable balance between nonlinear and dispersive effects, are ubiquitous in nature: examples range from quantum mechanics to astrophysics [1,2]. Optical solitons, which provide a fundamental building block in mode-locked laser systems, are under intense research attention recently for their striking analogies with their matter molecule counterparts [3–5]. Specifically, several solitons coexist in the laser cavity, which results in the generation of soliton molecular complexes and supramolecular structures [6,7]. From a fundamental viewpoint, solitons are regarded as an excellent platform for exploring the particle-like nature of nonlinear waves, with analogies extending from fluid dynamics, plasmas, Bose-Einstein condensates, DNA mechanical waves and ocean's ghost waves [8–12]. Although laser soliton propagation can be theoretically described by means of a generalized nonlinear Schrödinger equation (GNSE) or a complex Ginzburg–Landau equation (CGLE), the initial self-starting state of the mode-locking process contains a rich variety of nonlinear, highly stochastic and non-repetitive phenomena. The analysis of the associated self-starting dynamics will require the development of new theoretical approaches, beyond the realm of the GNSE or CGLE.

Over the past few years, the self-starting dynamics of mode-locked lasers has been extensively studied, both experimentally and theoretically. Typical revealed phenomena include: raised relaxation oscillation, dominant wavelength component shift, spectral beating, bound states, modulation instabilities and soliton explosions. These have been studied in various cavity soliton build-up examples by means of the emerging time-stretch dispersive Fourier transform (TS-DFT) technique [13–17], which enables mapping spectral information into a time-domain waveform. Recently, the buildup processes of Kerr lens mode-locking in titanium sapphire lasers, and the entire buildup processes of conventional solitons (CSs) (that is, essentially resulting from a balance between dispersion and Kerr nonlinearity, as opposed to dissipative solitons, (DSs) which also require an additional balance between loss and gain) in mode-locked fiber laser have been reported [13]. Different routes to generating stable temporal CSs have been established. For a solid-state laser with a relatively short cavity, the CS formation process mainly includes initial Q-switched mode-locking (QML) fluctuations, wavelength shifting and transient spectral beating. Whenever the cavity length of the mode-locked fiber laser grows larger, polarization and

* Corresponding authors.
E-mail addresses: gaolei@cqu.edu.cn (L. Gao), zhutao@cqu.edu.cn (T. Zhu).

https://doi.org/10.1016/j.optlastec.2021.107677
Received 1 February 2021; Received in revised form 17 May 2021; Accepted 9 November 2021
Available online 17 November 2021

pump power fluctuation-induced pulse interactions between the coexisting solitons and dispersive waves occur. In this case, transient bound states may appear after the spectral beating stage, before the generation of a stable temporal CS trains [18]. The previous pathways have been explored, in order to identify the self-starting of CS mode-locked lasers in the absence of environmental perturbations. However, in fiber laser cavities, material dispersion, modal dispersion and long cavity lengths will fall act to intensify the interactions among solitons, or among solitons and dispersive-wave radiation, which results in the generation of various types of bound-states [19]. It has been reported that two bound soliton-pair molecules can form molecular complexes [6], or generate a supramolecular state via the self-assembly of a large number of optical solitons [7]. These bound states evolve as laser roundtrips grow larger, and form interference fringes within the spectrum in a 2D real-time spectrogram. On the other hand, spectral beating occurring in soliton formation frequently modulates the spectral intensity in different roundtrips. Therefore, a simultaneous occurrence of the two types of spectral behavior associated with the CS build-up process may occur. The question arises, whether there is any other type of CS build-up in fiber lasers?

In this Letter, we give a positive answer to this question, by providing an experimental evidence of a novel CS generation pathway. Solitons emerge from shaking soliton molecules, featuring simultaneous beating and binding of their spectral properties. It is worth to note that, in these molecular triplets, satellite solitons are orthogonal to each other in their state of polarization. The schematic diagram of our soliton triplets with two satellite pulses orthogonal to each other in polarization domain is shown as the Fig. 1(b) (The L represents the length of fiber, and the $\tau 1$, $\varphi 1$ and $\tau 2$, $\varphi 2$ are the relative time interval and relative phase between satellite soliton 1, satellite soliton 2 and main soliton. The dashed arrows indicate the Cartesian coordinate system. Therefore, the polarization directions of the three soliton pulses lie in the XOY plane indicated by the red solid arrows. Here, we assume that the electric field of the main soliton vibrates in a positive Y-direction. The relative phase between satellite and main pulses evolves in a chaotic manner. The observed evolution of soliton molecules may provide a new insight into their internal dynamics, which is characterized by three degrees of freedom: relative phase, time interval, and state of polarization, which provides a new insight in the dynamical process of CS formation.

2. Experimental setup

The schematic diagram of our fiber laser is shown in Fig. 1(a). 1 m erbium-doped fiber (E08-A352A-01-1B22) with a dispersion coefficient of ~ -20 ps2/km is used as the gain medium. 7.8 m SMF has a dispersion coefficient of ~ –22.9 ps2/km. A polarization controller (PC) is inserted into the cavity to regulate the mode-locking operation. The isolator (ISO) is used to ensure unidirectional pulse propagation. We employ a 980/1550 nm wavelength division multiplexer (WDM) to couple the 980 nm pump laser. Finally, a 90/10 coupler is used as output device. The saturable absorber is a homemade single wall carbon nanotube film (SWCNT) [20]. To facilitate the observation of the buildup process of a CS, we added a mechanical chopper in front of the 980 nm pump laser.

The laser single-shot spectra was characterized by means of a homemade TS-DFT, where periodic signals are linearly stretched by a 510 m dispersion compensation fiber (DCF) (with dispersion of about −400 ps/nm/km) for frequency-to-time transformation, and subsequently fed to a 50 GHz photodiode (PD) connected to a real-time oscilloscope (Tektronix, DSA 72004B) with 20 GHz bandwidth. The spectral resolution of DFT measurement is 0.25 nm. Which can be calculated according to the formula: $\Delta\tau = |D| \cdot L \cdot \Delta\lambda$, where $\Delta\lambda$ is the bandwidth of the spectrum, D is the group delay dispersion per unit length of the dispersive element (usually in ps/nm/km), and $\Delta\tau$ is the temporal duration of the spectral mapping. The time trace of the laser output was also recorded by a 20 GHz PD, fed to another channel of the real-time oscilloscope.

This powerful real-time spectroscope TS-DFT also has two shortcomings, the first one is that when the ultrafast fiber laser cavity operates in a multi-soliton state (especially the time interval of pulses is serval nanosecond, and the soliton molecules cannot be formed), the real-time spectra observed on the oscilloscope will overlap and the results will be inaccurate. However, when the number of soliton is small and the soliton molecules are formed, the real-time spectrum of every roundtrip measured by TS-DFT is a single spectrum with interference envelope formed by the whole soliton molecules [5,6], whose spectral results will be inaccurate. The second problem is that because TS-DFT technology requires input condition of the signal is confined to short pulses, the continuous wave / quasi-continuous wave (CW/QCW) output from ultrafast fiber laser cavity cannot be measured. However, during the mode-locking build-up process, especially during the relaxation oscillation process usually accompanied by such CW/QCW components. To face this problem, we can actually combine the parametric spectro-temporal analyzer (PASTA) technology to resolve the spectral information of CW/QCW components [21].

3. Experimental results and discussion

Self-starting of mode-locking occurs at a pump power of 75 mW. A train of fundamental CS with a 3-dB spectral bandwidth of 4 nm, pulse duration of ~ 700 fs and time period of ~ 44 ns is generated. By utilizing the chopper to switch on and off the pump, we are able to continuously observe the CS build-up process. By combining the TS-DFT system with the fast-acquisition functionality of the real-time oscilloscope, we recorded the entire relaxation oscillation process associated with CS formation on its screen. As a result of properly adjusting the state of the PC in our experiments, a new process of CS generation emerged, alongside other pathways [18].

The details of this CS formation process, as obtained by the TS-DFT method, are shown in Fig. 2(a). Its general features are similar to

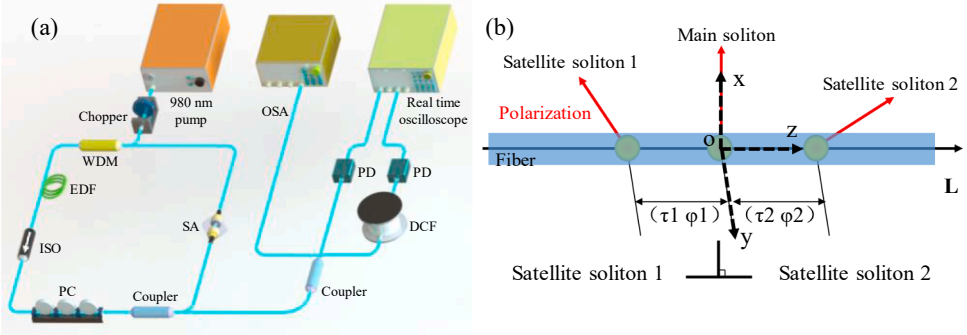

Fig. 1. (a) Schematic diagram of the fiber laser. (b) Schematic diagram of a visual representation of soliton triplets with two satellite pulses orthogonal to each other in polarization domain.

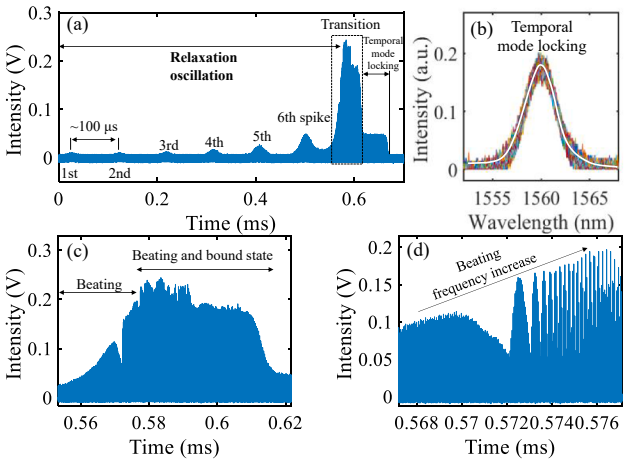

Fig. 2. (a) Original single-shot spectral data of laser buildup dynamics detected by the TS-DFT system. (b) Superimposed single-frame spectra of 100 roundtrips of mode-locked laser output. The white tracks are the average spectrum. (c) The local enlargement of the transient pulse in Fig. 2(a). (d) Local enlargement of the intensity beating region in Fig. 2(c).

previously reported, SWCNT-based SA, build-up processes of CSs, soliton molecules, and DSs. As can be seen in Fig. 2(a), a first laser spike appears after the accumulation of sufficient population inversion in the gain medium. Subsequently, relaxation oscillations occur with a laser spike separation of ~ 100 μs, which corresponds to the gain oscillation of the EDFs. Then, after six consecutive laser spikes, population inversion in the EDF reaches its peak value. As a result of the associated large amplification, a transient high peak power pulse is generated, which is subject to self-phase modulation leading to an abrupt spectral broadening. By zooming in the transient pulses as shown in Fig. 2(c), we may identify a first region of intensity beating, followed by a region of coexisting spectral beating and binding. The initial intensity evolution in the transient pulse is similar to that reported in the first CS formation pathway of Ref. 18. In Fig. 2(d), we can clearly see that the beating frequency increases over time. This phenomenon was already reported in the build-up process of Kerr lens mode-locking in solid-state lasers [13]. After a ~ 40 μs transition state, temporal mode-locking is established. Fig. 2(b) depicts the superimposed single-frame spectra of 100 roundtrips of laser output. The 3-dB bandwidth of the temporal CS is approximately 4 nm, which is equivalent to that resulting from the average spectrum, as obtained by the OSA.

The trend of intra-cavity energy evolution during the CS formation process is shown in Fig. 3(a) by integrating the single-shot spectra of each round-trip. The intra-cavity energy evolves in five separate stages. In the first stage (1), energy raises because of the accumulation of

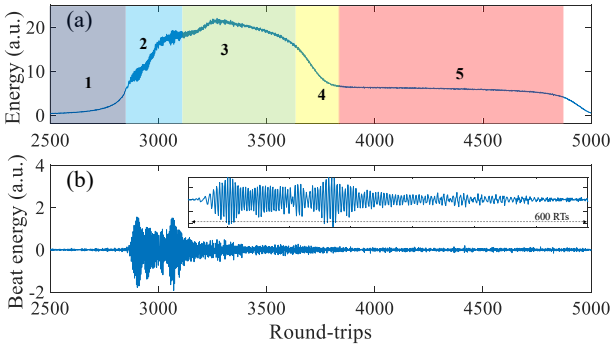

Fig. 3. (a) Energy evolution of transition and temporal mode locking stages. (b) Details of damping of energy jitter. The inset is an enlarged view of the 600 roundtrips, where damping of energy jitter occurs.

population inversion in gain medium. Subsequently, with the occurrence of beating (2), small amplitude oscillations or jitter accompany a rapid increase of the energy. Immediately after that, gain gradually reaches saturation, which damps the laser energy jitter, while average value of intra-cavity energy gradually decreases (3). The disappearance of jitter precedes the occurrence of stable temporal mode-locking: before that, energy rapidly declines (4) until it stabilizes (5). And it's worthy to notice that the normalized energy of stage 5 (temporal mode locking regime) is about 6 to 7. The max energy of laser during the buildup process is about third times than stage 5. We will further discuss that by calculating the evolution of first-order autocorrelation trajectories of laser output. In order to amplify the damping of energy jitter, we smoothed the energy curve of Fig. 3(a) and computed the difference of the original data and smooth curve for the energy evolution: the result is shown in Fig. 3(b). Here the inset shows an enlarged view of 600 roundtrips, over which the damping of energy jitter mainly occurs. We can clearly see that the frequency of energy beating increases at first, next it stabilizes, and finally it maintains a stable beating frequency while its amplitude gradually declines. The trend of frequency variation of the cavity energy beating is similar to what reported in Ref. [13].

Furthermore, we divided the recorded real-time signal into separate intervals, with a duration equal to the average cavity round-trip time of 44 ns. All intensities were normalized with respect to the maximum value in the whole buildup process. The first recorded pulse is determined by the triggering level of the real-time oscilloscope during TS-DFT detection. In other words, the oscilloscope records the pulse from the laser cavity, which is created by the first relaxation oscillation. Fig. 4(a) shows original data of the sixth spike of relaxation oscillation of the laser, followed by soliton formation. Fig. 4(b) displays the entire complex process of CS generation, involving a Q-ML stage, initial spectrum broadening, spectral beating, soliton molecule (bound state) formation, and a final temporal mode-locking state involving a single-soliton generation. The insert figure show the partial enlarged detail of that interesting regime consisted of the complex soliton dynamics. As we can see from the real-time spectra, in the transition stage spectral intensity beating appears as the number of roundtrips increases. At the same time, interference fringes appear within the spectrum, meaning that soliton molecules are generated. To our knowledge, this phenomenon has been observed here for the first time in a laser cavity soliton formation process. As a matter of fact, previous experiments reported two different CS formation processes in a fiber laser [17,18]. One pathway included the growth of relaxation oscillations, followed by the QML stage, spectral beating, and finally stable single-soliton mode-locking. The other pathway included an extra transient bound-state stage (soliton molecules) between the single-pulse mode locking operation and the beating stage. The buildup process observed in Fig. 4 provides a third pathway, which complements the dynamics of passive mode locking soliton formation.

To better understand the dynamics of the CS generation processes, we show in Fig. 5 the evolution of the pulse, its spectrum, and the temporal separation between molecular pulses. Because of the 50 ps temporal resolution (The detection system contained high speed PD and oscilliscope have a bandwidth of 20 GHz.) of the direct measure of the pulse intensity, it is impossible to observe satellite pulses generated during the transition stage in Fig. 5(a). However, we can see that the pulse energy associated with the transition stage is much higher than that of steady ML state, which is corresponding to the energy curve of Fig. 3(a) obtained by integrating the single-shot spectra of each roundtrip. For the CS laser cavity, the pulse intensity is clamped, hence it cannot be increased further. On the other hand, we aim at investigating the possibility of soliton splitting during the transition stage. Therefore, we performed a Fourier transform of every single-shot spectrum, in order to obtain the field autocorrelation of the transition stage as shown in Fig. 5(d). Via the initial beating process, a single soliton is broken into two, illustrating the main pulse separating to two pulses from roundtrip 2930 till roundtrip 3090. Go back to Fig. 3(a), we find that the

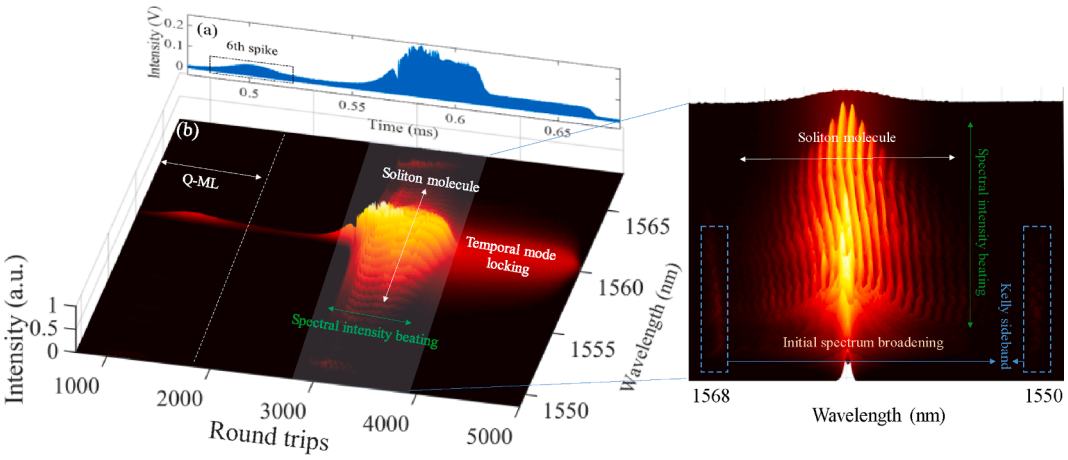

Fig. 4. (a) Original intensity data of the sixth relaxation oscillation of the laser, and the entire process of soliton formation. (b) Experimental real-time observation during the formation of a soliton. The insert figure is the partial enlarged detail of that interesting regime consisted of the complex soliton dynamics.

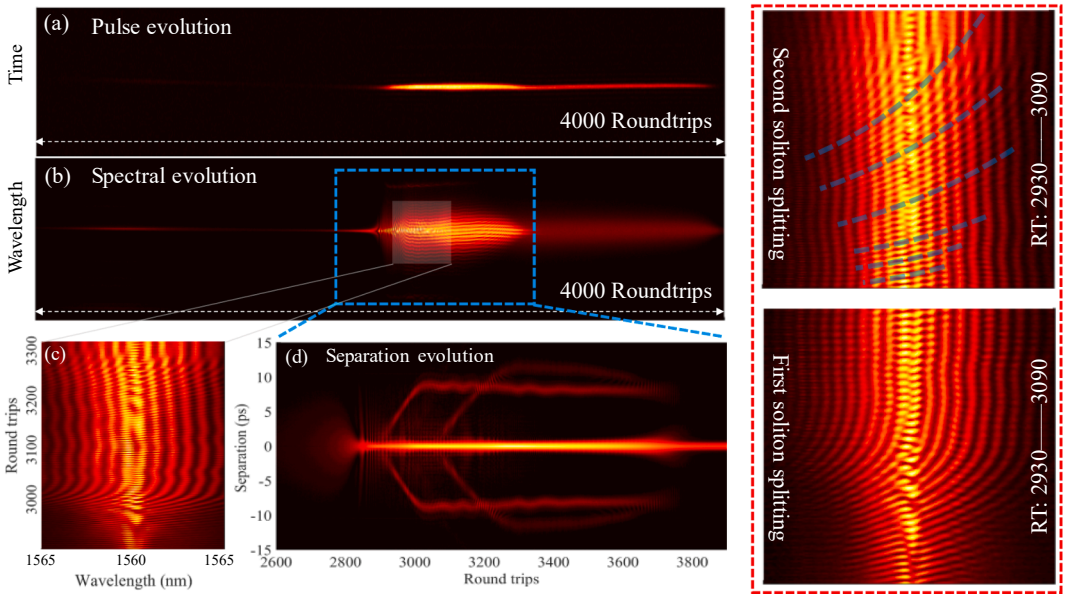

Fig. 5. (a) Time trace of the output laser. (b) 2D real-time spectra of the output laser from 6th relaxation oscillation to the temporal mode locking state. (c) Spectral close-up. (d) The first-order autocorrelation trajectory of the whole transition stage of Fig. 5(b). The bottom insert figure is the real time spectrum at the first pulse split. The top insert figure is the real time spectrum at the second pulse split. The blue transparent dotted line is the evolution trend of the newly generated interference fringe.

normalized energy of laser at 2930 is about 13, which is about two times than the normalized energy of stage 5 (temporal mode locking regime). The energy variation observed here corresponds to the second stage of Fig. 3(a). Owing to the pulse-shaping mechanism in the cavity with anomalous dispersion, the soliton amplitude remains quantized [22]. As a result of the overall energy growth in the cavity, the soliton splits and forms a molecular pair of solitons. From Fig. 3 (b), we can see that in this stage the cavity energy is violently oscillating caused by the energy flowing between the soliton molecule, and the frequency of energy beating increases with the number of roundtrips. Actually, this beating dynamic occurs at the transition from Q-ML to stable mode-locking is known as 'auxiliary pulse mode-locking' [13]. However, in our discussed case, there is a little different. From Fig. 3(b) and Fig. 5(d), it can be seen that the beginning of energy jitter and the first split of the main pulse both occur at the roundtrips of 2930. Therefore, there are two pulses in the cavity at this time, and the intensities of the two pulses are different in the initial stage of splitting, so the effective refractive index felt by them is different due to nonlinearity. So that the two pulses occur temporal walk-off which accumulates over many roundtrips. When they meet again, constructive or destructive interference occurs according to their accumulated relative phase. Therefore, this spectral intensity beating changes as roundtrips increase. The modulation period should be an integer multiple of roundtrips, so it will change fast. In our case, the intensity of split pulse is at the same order of magnitude as the original pulse, which can be estimated from the 1st-order autocorrelation trajectory, the intensity modulation will be stronger when the intensity is similar.

Moreover, this energy beating will induce the jitter relative phase in the same trend. In other words, the higher energy pulse in the soliton molecule accumulates more nonlinear phase shifts, the more violent energy flowing causes the more violent relative phase jitter [23]. In the corresponding 2D real-time spectrum (the bottom insert figure of Fig. 5), we can see that the longitudinal spectral intensity beating grows substantially deeper as the roundtrips increase from 2930 to 3090. Therefore, we may conjecture that shaking soliton pairs are formed in this stage of the CS generation process [19]. And because of the existing of

spectral intensity beating, more complex relative phase changes are introduced.

Next, as can be seen in the third stage of Fig. 3 (a), solitons recirculating in the laser cavity continue to be amplified by gain medium. When normalized energy beyond 18 (three times than normalized energy of stage 5) at roundtrips of 3090 in Fig. 3(a), new autocorrelation peaks are generated at the same roundtrips of 3090 observed from Fig. 5 (d). As a result, a pulse in the molecular pair splits again, which leads to a triplet shaking soliton molecular structure and have been firstly experimentally observed in soliton molecules. The corresponding spectral evolution and autocorrelation trajectory appear in the top insert figure of Fig. 5 and Fig. 5 (d), respectively. Here we define the pulse in the middle of the triplets as the main pulse, and the left and right sides as the satellite pulses. By tracking the relative time interval between the satellite solitons and the main central pulse of the triplet, one obtains the curves in Fig. 6(a): as can be seen, the time interval between satellite soliton 1 and the main pulse (blue curve) differs from that between satellite soliton 2 and main pulse (red curve). As a consequence, the autocorrelation trace of the triplet-style soliton molecule should exhibit seven peaks [24]. However, Fig. 5(d) only shows five autocorrelation peaks. The missing autocorrelation peaks are formed by the coherent interaction of the two satellite pulses. Since our spectral resolution of DFT-based real-time spectroscopy is 0.25 nm, which corresponds to the maximum autocorrelation time range is 50 ps. This is because the denser spectral interference fringes mean the bigger temporal interval of soliton molecule [6]. The separations between the two satellite pulses and main pulse are less than 20 ps, as can be seen from Fig. 6(a). So resolution of our system is enough to detect the interference spectral characteristic of the two satellite pulses.

Corresponding to the method of Ref. [6], we can get the time interval and relative phase between pulses in each roundtrip by tracking the side peaks in Fig. 5(d) and calculating the argument. In order to describe the complex dynamics of the soliton triplet we must include the rest degrees of freedom, relative phase and the state of polarization. The waveguides utilized in our cavity are not able to support different mode fields, so there is no need to discuss the mode fields of soliton molecules knowns as spatial–temporal mode locking as a degree of freedom. Then, we firstly think about relative phase. When the relative phase of the two satellite pulses is an odd multiple of π, their spectra will be destructively superimposed when they meet. But from the method of Ref. [6], we can see, the relative phase just influences the argument of side-peak of first order autocorrelation instead of amplitude. So, the reason of forming Fig. 5(d) can only be analyzed from the perspective of polarization. We think about that situation. When satellite soliton 1 and satellite soliton 2 are orthogonal to each other in polarization domain, i.e., the two satellite solitons are incoherent. There is no interference generated by the interaction of satellite pulses in Fig. 5b. Then the first-order autocorrelation trace of the triplet soliton molecule will only exhibit five peaks.

Furthermore, we trace the position of the autocorrelation peak generated by the two satellite pulses and the main pulse shown as Fig. 6 (a), and then calculate the argument of these two peaks' position of every roundtrip. The calculated argument is the relative phase of soliton molecule, and the temporal position of autocorrelation peak is the relative temporal interval. So, the relative phase of the satellite pulses and the main pulse can be solved [6]. Fig. 6(b) and 6(c) illustrate the chaotic evolutions of the relative phase between the two satellite pulses and the main pulse. The trajectory of the chaotic internal motions in the soliton triplet interaction space are shown in Fig. 6(d)-6(g). The parameters τ and φ are the time interval and relative phase between satellite solitons and main soliton. The relative phase evolution of the two satellite pulses differs from that of shaking soliton pairs with chaotically evolving phase oscillations as reported in reference [25]: here the chaotic dimension appears to be of a higher level. The present increased degree of chaos may be due to the increased dimensionality of the parameter space associated with the evolution of the relative phase, the energy flow within the soliton molecules, and state of polarization. As a result, the shaking soliton molecules that formed in the process of CS generation exhibit intensity fluctuations within each polarization component which are more chaotic than that in Ref. [25]. What's more, our entire soliton molecular evolution is forming during the establishing process of laser under the unstable cavity energy situation accompanied by the strong spectral intensity beating, which can intensify the energy flowing between the soliton molecule. As can be seen in Fig. 6, here the relative phase evolve in a completely chaotic fashion.

Therefore, this triplet-soliton molecule has 5 autocorrelation peaks that can only be understood from the polarization domain. This could be speculated by energy and momentum conservation considerations: the main pulse of the triplet soliton molecule splits its energy among its two

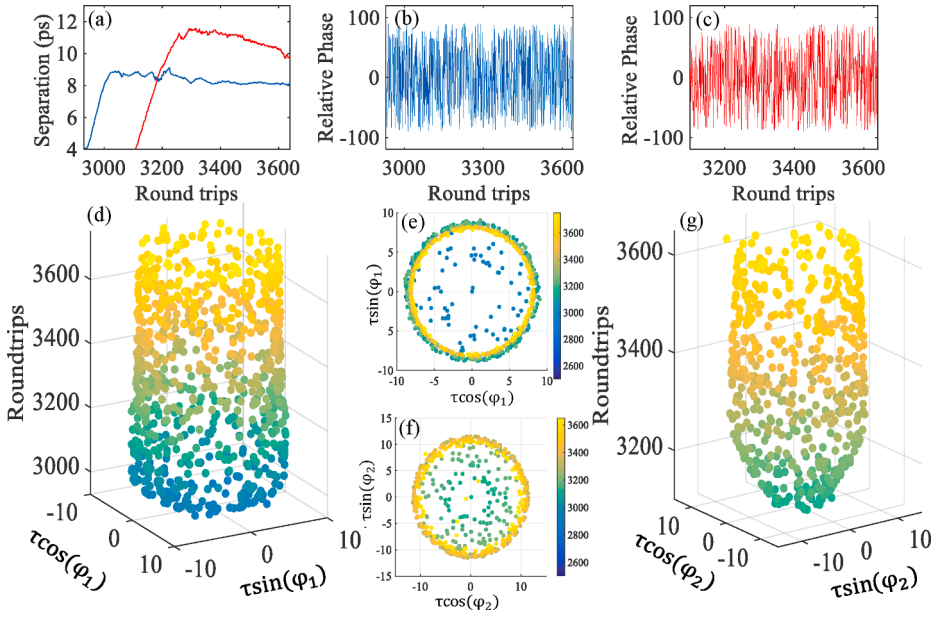

Fig. 6. (a) Temporal separation of the satellite soliton 1 and main pulse (blue curves), the satellite soliton 2 and main pulse (red curves). (b) and (c): relative phase between satellite soliton 1 or satellite soliton 2 and the main pulse, respectively. (d)-(e) and (f)-(g): Trajectories of chaotic internal motions of satellite soliton 1 and satellite soliton 2 in the interaction space.

orthogonal polarization components, leading to a pair of mutually perpendicular satellite pulses. Finally, as the population inversion is reduced and gain saturates, the intra-cavity energy rapidly decreases, as shown in the second half of the third stage and the fourth stage of Fig. 3 (a). As a result, the main pulse in the cavity no longer splits its energy into its two orthogonal polarizations, so that the two satellite pulses gradually decay and disappear from the cavity. Eventually, only the main pulse survives, forming a stable mode-locked state.

4. Conclusion

We experimentally observe a novel dynamics of CS formation, facilitated by orthogonally polarized shaking soliton molecules. By analyzing the evolution of the three molecular degrees of freedom, namely their relative time interval, relative phase, and polarization state, we revealed the presence of a fully developed chaotic internal motion of shaking soliton molecule triplets in the interaction space. We believe that the increased internal-motion chaos results from the extra degree of freedom associated with the orthogonally polarized satellite soliton pairs in this shaking soliton triplets and spectral intensity beating introduced in the process of soliton build-up. The complex internal dynamics of the soliton molecule is governed by the subtle energy flow between each individual constituent, facilitated by gain dynamics and soliton interactions. The internal energy flow in soliton molecules obeys energy and momentum conservation, which explains the splitting of two orthogonally polarized satellite pulses from the main pulse. Our findings shed a new light in the internal dynamics of soliton molecules with higher degrees of freedom, and provide a complementary route to process soliton-based laser mode-locking.

Funding

Natural Science Foundation of China (62075021, 61635004, 61705023), Graduate scientific research and innovation foundation of Chongqing, China (CYB19037), National Science Fund for Distinguished Young Scholars (61825501). European Research Council (740355). Russian Ministry of Science and Education (14.Y26.31.0017).

CRediT authorship contribution statement

Yulong Cao: Writing – original draft. **Lei Gao:** Writing – review & editing. **Stefan Wabnitz:** Writing – review & editing. **Zhiqiang Wang:** Writing – review & editing. **Qiang Wu:** Data curation. **Lingdi Kong:** Data curation. **Ziwei Li:** Data curation. **Ligang Huang:** Data curation. **Wei Huang:** Data curation. **Tao Zhu:** Supervision.

Declaration of Competing Interest

The authors declare that they have no known competing financial interests or personal relationships that could have appeared to influence the work reported in this paper.

References

[1] J.R. Anglin, W. Ketterle, Bose-Einstein condensation of atomic gases, Nature 416 (6877) (2002) 211–218.
[2] G.A. Mourou, T. Tajima, S.V. Bulanov, Optics in the relativistic regime, Rev. Mod. Phys. 78 (2) (2006) 309–371.
[3] J.W. Fleischer, M. Segev, N.K. Efremidis, D.N. Christodoulides, Observation of two-dimensional discrete solitons in optically induced nonlinear photonic lattices, Nature 422 (6928) (2003) 147–150.
[4] M. Stratmann, T. Pagel, F. Mitschke, Experimental observation of temporal soliton molecules, Phys. Rev. Lett. 95 (14) (2005), 143902.
[5] G. Herink, F. Kurtz, B. Jalali, D.R. Solli, C. Ropers, Real-time spectral interferometry probes the internal dynamics of femtosecond soliton molecules, Science 356 (6333) (2017) 50–54.
[6] Z.Q. Wang, K. Nithyanandan, A. Coillet, P. Tchofo-Dinda, P. Grelu, Optical soliton molecular complexes in a passively mode-locked fibre laser, Nat. Commun. 10 (2019) 830.
[7] W. He, M. Pang, D.H. Yeh, J. Huang, C.R. Menyuk, P.S. Russell, Formation of optical supramolecular structures in a fibre laser by tailoring long-range soliton interactions, Nat. Commun. 10 (2019) 5756.
[8] H. Hasimoto, Soliton on a vortex filament, J. Fluid Mech. 51 (FEB8) (1972) 477.
[9] E. Kuznetsov, A. Rubenchik, V.E. Zakharov, Soliton stability in plasmas and hydrodynamics, Phys. Rep. 142 (1986) 103–165.
[10] K.E. Strecker, G.B. Partridge, A.G. Truscott, R.G. Hulet, Formation and propagation of matter-wave soliton trains, Nature 417 (6885) (2002) 150–153.
[11] C.B. Tabi, A. Mohamadou, T.C. Kofane, Soliton-like excitation in a nonlinear model of DNA dynamics with viscosity, Math. Biosci. Eng. 5 (1) (2008) 205–216.
[12] D.R. Solli, C. Ropers, P. Koonath, B. Jalali, Optical rogue waves, Nature 450 (7172) (2007) 1054–1057.
[13] G. Herink, B. Jalali, C. Ropers, D.R. Solli, Resolving the build-up of femtosecond mode-locking with single-shot spectroscopy at 90 MHz frame rate, Nat. Photonics 10 (5) (2016) 321.
[14] X.M. Liu, X.K. Yao, Y.D. Cui, Real-time observation of the buildup of soliton molecules, Phys. Rev. Lett. 121 (2) (2018), 023905.
[15] J. Peng, H. Zeng, Build-up of dissipative optical soliton molecules via diverse soliton interactions, Laser Photonics Rev. 12 (8) (2018) 1800009, https://doi.org/10.1002/lpor.v12.810.1002/lpor.201800009.
[16] A.F.J. Runge, N.G.R. Broderick, M. Erkintalo, Observation of soliton explosions in a passively mode-locked fiber laser, Optica 2 (1) (2015) 36–39.
[17] Y.D. Cui, X.X. Liu, Revelation of the birth and extinction dynamics of solitons in SWNT-mode-locked fiber lasers, Photonics Res. 7 (4) (2019) 423–430.
[18] X. Liu, Y. Cui, Revealing the behavior of soliton buildup in a mode-locked laser, Adv. Photonics 1 (01) (2019) 1, https://doi.org/10.1117/1.AP.1.1.016003.
[19] J.M. Soto-Crespo, P. Grelu, N. Akhmediev, N. Devine, Soliton complexes in dissipative systems: Vibrating, shaking, and mixed soliton pairs, Phys. Rev. E 75 (1) (2007), 016613.
[20] Y. Cao, L. Gao, Y. Li, J. Zhang, F. Li, T. Zhu, Graphene-based all-optical multi-parameter regulations for an ultrafast fiber laser, Opt. Lett. 43 (18) (2018) 4378–4381, https://doi.org/10.1364/OL.43.004378.
[21] X. Wei, B. Li, Y. Yu, C. Zhang, K.K. Tsia, K.K.Y. Wong, Unveiling multi-scale laser dynamics through time-stretch and time-lens spectroscopies, Opt. Express 25 (23) (2017) 29098, https://doi.org/10.1364/OE.25.029098.
[22] Z. Wang, K. Nithyanandan, A. Coillet, P. Tchofo-Dinda, P. Grelu, Buildup of incoherent dissipative solitons in ultrafast fiber lasers, Phys. Rev. Res. 2 (1) (2020), 013101.
[23] K. Krupa, K. Nithyanandan, U. Andral, P. Tchofo-Dinda, P. Grelu, Real-time observation of internal motion within ultrafast dissipative optical soliton molecules, Phys. Rev. Lett. 118 (24) (2017), https://doi.org/10.1103/PhysRevLett.118.243901.
[24] Y. Luo, R. Xia, P.P. Shum, W. Ni, Y. Liu, H.Q. Lam, Q. Sun, X. Tang, L. Zhao, Real-time dynamics of soliton triplets in fiber lasers, Photonics Res. 8 (6) (2020) 884–891.
[25] R. Xia, Y.Y. Luo, P.P. Shum, W.J. Ni, Y.S. Liu, H.Q. Lam, Q.Z. Sun, X.H. Tang, L. M. Zhao, Experimental observation of shaking soliton molecules in a dispersion-managed fiber laser, Opt. Lett. 45 (6) (2020) 1551–1554.